Dynamics of Compact Objects

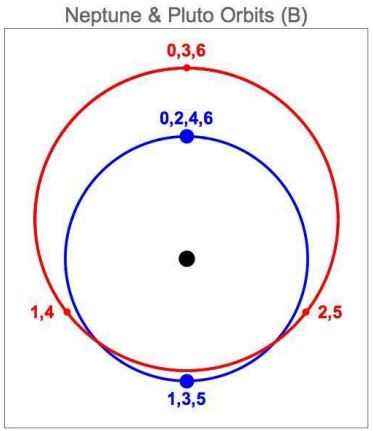
Some celestial-mechanical effects on hierarchical orbits

Naoki Seto (Kyoto University)

2020.2.27 Waseda Univeristy

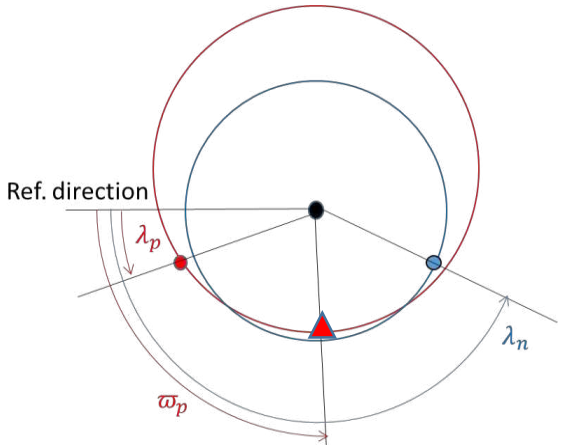
Introduction-why hierarchical orbit?

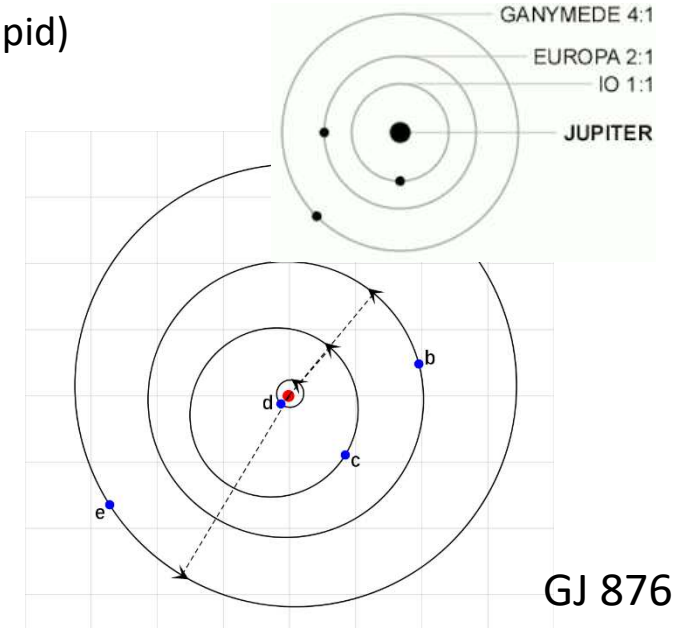
- Various resonant dynamics in planet/satellite systems
- Mean motion resonances
  - nearly commensurable relations between orbital periods
  - Sun-Neptune-Pluto (3:2) $3\lambda_p - 2\lambda_n - \varpi_p \sim const$
  - GJ 876 (4:2:1), Galilean satellites (4:2:1)
  - …



$\lambda_{n,}\lambda_p$: instantaneous direction (rapid)

ϖ_p: pericenter direction (slow)



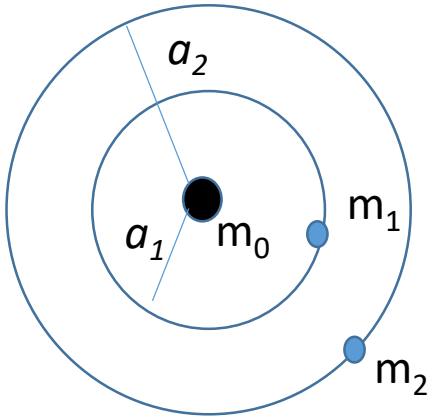


GJ 876

- Mass limit for mean motion resonances
  - Orbital stability for nearly circular orbits (Gladman 93)

resonance	$(m_1+m_2)/m_0$
3:2	0.0018
5:3	0.0037
2:1	0.010
5:2	0.026

Lee et al. 09



Suzuki-san's talk

$m_0 \gg \max[m_1, m_2]$ for standard mean motion resonances (e.g. planetary system)

In this talk

$m_0 \sim \max[m_1, m_2]$ is allowed for a large orbital hierarchy $(\alpha \equiv \frac{a_1}{a_2} \ll 1)$

1: inner orbit
2: outer orbit

Outline

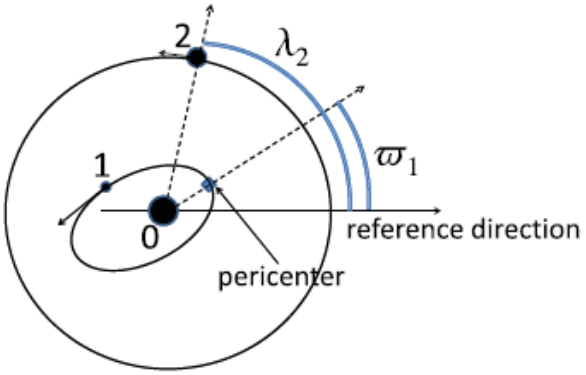
- A special mean motion resonance for $m_0 \sim \max[m_1, m_2]$
- Kozai-Lidov mechanism
  - Basic aspects with “averaged” Hamiltonian
  - Recent studies
    - Realizing highly eccentric orbits (e.g. for rapid evolution)
    - Activate large eccentricity amplification after binary evolution
    - 3-body systems in dense star clusters
- Summary

1:0 resonance for $m_0 \sim \max[m_1, m_2]$

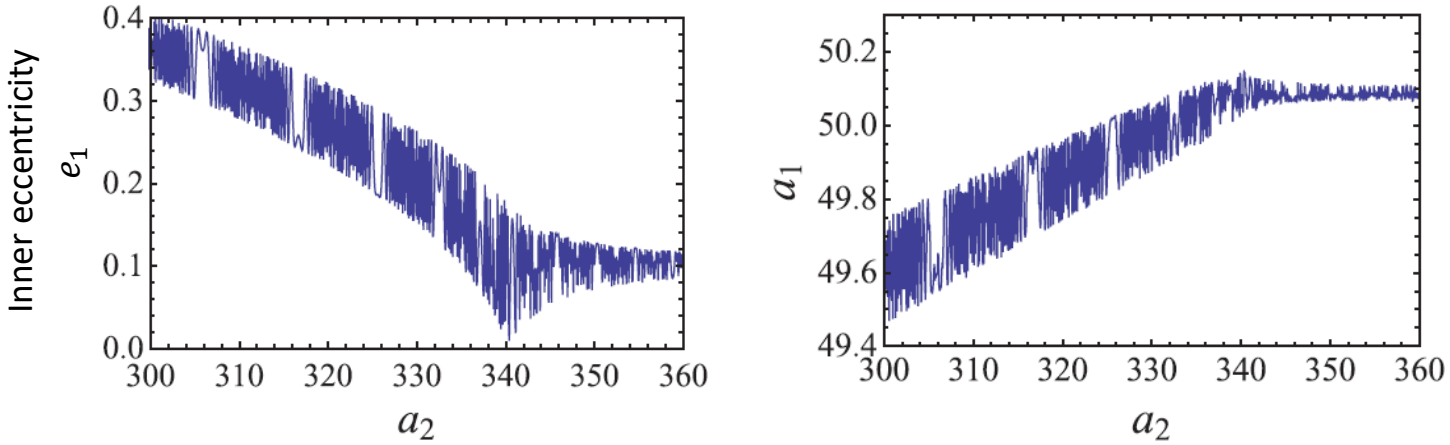
Seto 2013

- PN direct calculation for (MBH+star)+MBH

m_0=0.9, m_1=0, m_2=0.1, a_1=50, a_2=360, e_1=0.1, e_2=0 (G=c=M_{total}=1)

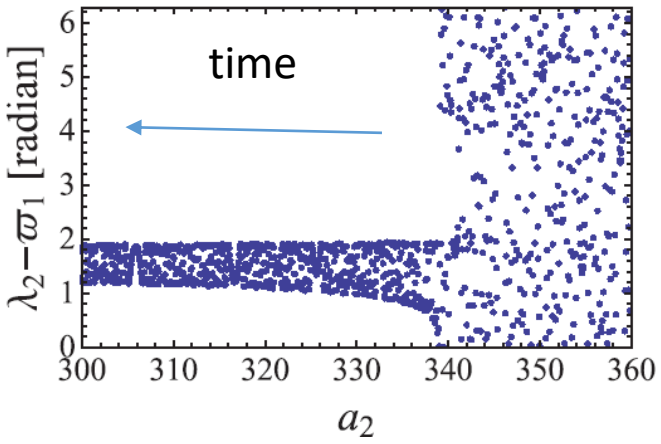


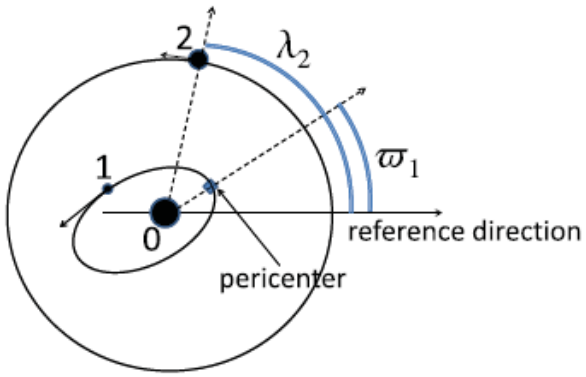
Outer orbital decay by GW emission



Outer semi-major axis (decreasing time coordinate)

Inner orbit starts to interact strongly with outer orbit at a_2=340





- Captured into a resonant state with $\lambda_2 - \varpi_1 = 1\lambda_2 - 0\lambda_1 - \varpi_1 \sim \pi/2$

  Technically 2:0 (≠1:0) considering the shape of the dominant potential mode

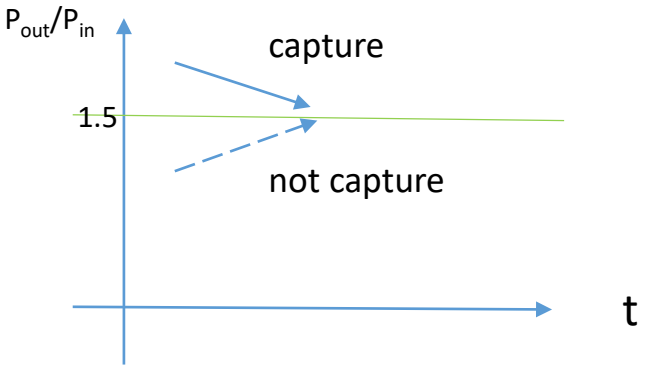
- Inner precession $\dot{\varpi}_1$: induced by 1PN effect

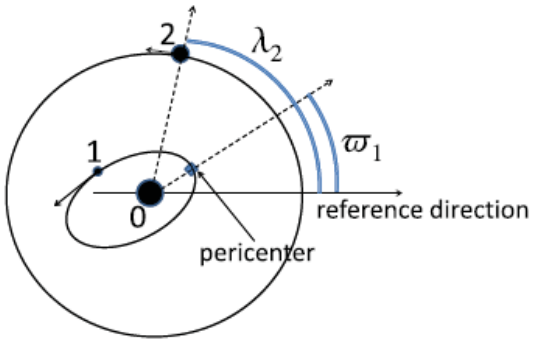
$$T_{1PN} \sim \frac{P_1(1-e_1^2)}{3}\left(\frac{G(m_1+m_0)}{a_1 c^2}\right)^{-2}$$

$$\left(\frac{v_1}{c}\right)^{-2} \text{ (PN parameter)}^{-1} \Rightarrow \alpha = \frac{a_1}{a_2} \sim \left(\frac{v_1}{c}\right)^{4/3}$$

$$P_2 = P_1 \underbrace{\left(\frac{a_1}{a_2}\right)^{-\frac{3}{2}}}_{\alpha} \left(\frac{\mathrm{m}_0+\mathrm{m}_1}{m_0+m_1+m_2}\right)^{1/2}$$

- Resonant state $\lambda_2 - \varpi_1 \sim const$
  - $m_0 \sim m_1 \sim m_2$ allowed?
    - MMR capture: relatively approaching orbits (Murray & Dermott 00)
      - e.g capture into 3:2, P_{out}/P_{in} from 1.6 (not from 1.4)





    - No with orbital decay by GW emission

$$T_{GW} \sim \frac{a^4}{m_0 m_1 (m_0 + m_1)} \qquad \rightarrow m_1 \ll m_2$$

Gap for e_1

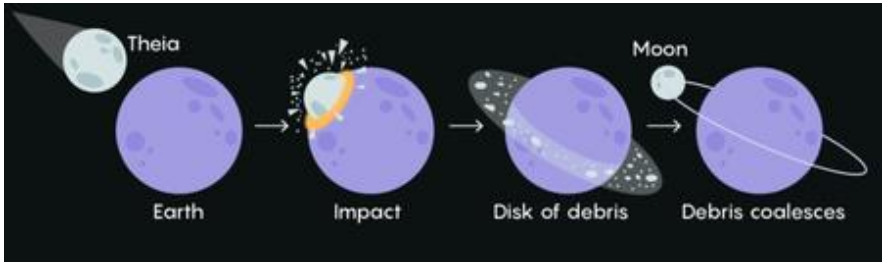
    - Possible with other migration process (relatively approaching)

$\lambda_{Sun} - \varpi_{moon} \sim const$ for Earth- Moon system

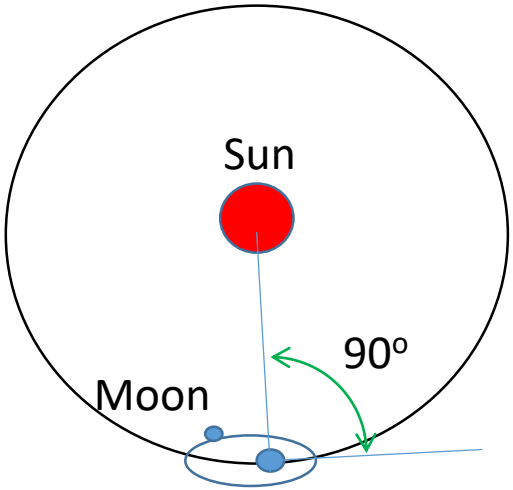
Evection resonance

Cuk & Stewart 12, Touma & Wisdom 98

- Giant impact scenario for Moon formation
  - Too much angular momentum?



- Transport 50% of angular momentum from Earth-Moon to Earth-Sun



$\lambda_{Sun} - \varpi_{moon} \sim \pi/2$

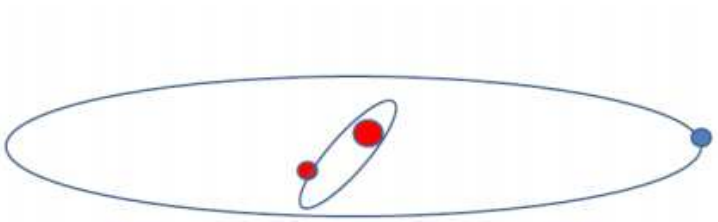
Precession by deformation of Earth

Outline

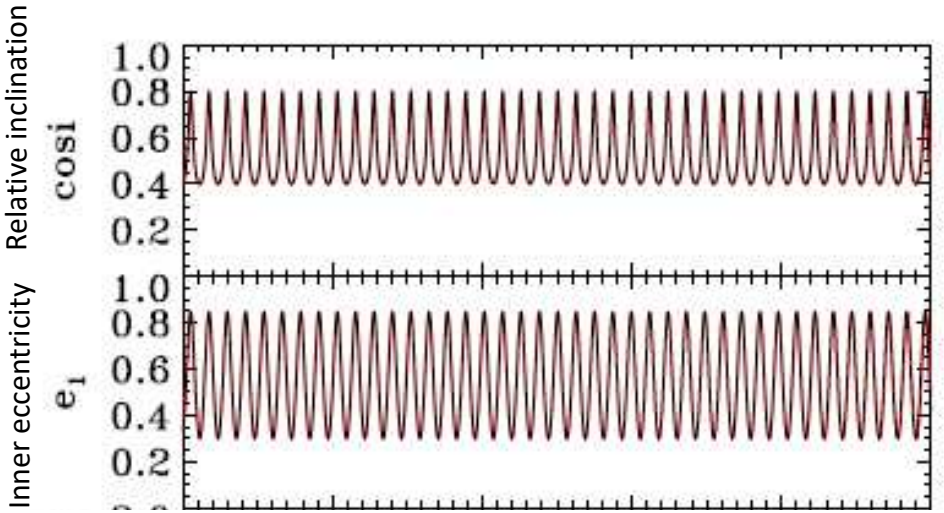
- A special mean motion resonance for $m_0 \sim \max[m_1, m_2]$
- Kozai-Lidov mechanism
  - Basic aspects with “averaged” Hamiltonian
  - Recent studies
    - Realizing highly eccentric orbits (e.g. for rapid evolution)
    - Activate eccentricity amplification along with binary evolution
    - 3-body systems in dense star clusters
- Summary

Kozai-Lidov mechanism

- Hierarchical inclined three-body system
- Oscillations of inner eccentricity and inclination



Large e_1 & cos I $\leftrightarrow$ Small e_1 & cos I



Black: Direct 3-body calculation

Figure 1. Comparison between our modified FEWBODY code (black) and an octupole-order secular code (red; Blaes et al. 2002). The triple system has $m_0 = 7.0\,M_\odot$, $m_1 = 6.5\,M_\odot$, $m_2 = 6\,M_\odot$, $a_1 = 10$ AU, $a_2 = 250$ AU, $e_1 = 0.3$, $e_2 = 0.1$, $g_1 = 0°$, $g_2 = 0°$, and cos $i = 0.4$. There is a good agreement between the calculations but there is a slow drift in $g_1 - g_2$. Figure discussed in Section 2.

Shappee & Thompson 19

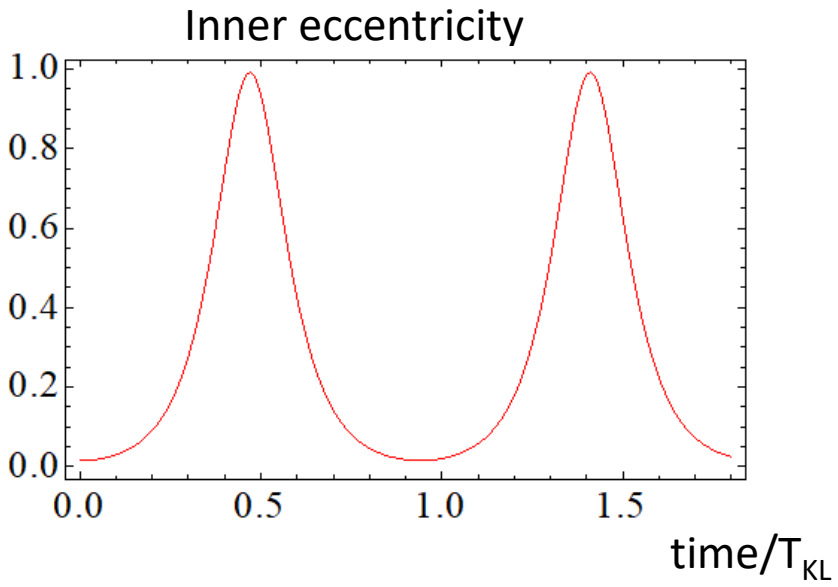
- Time scale of oscillation

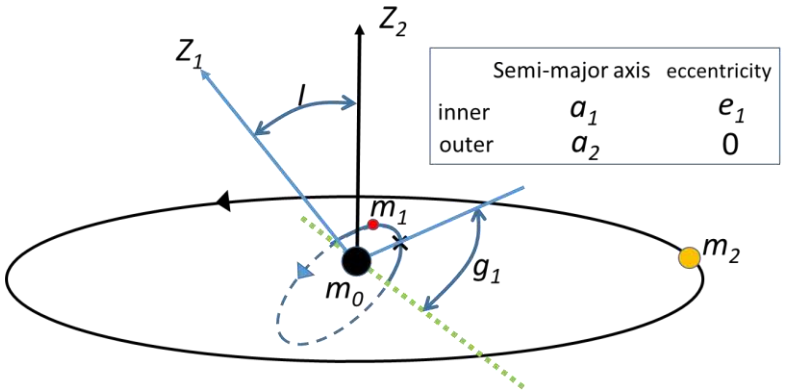
$$L_1 \sim \sqrt{G m_b a_1}$$

$$\frac{dL_1}{dt} \sim \frac{G m_2 a_1}{a_2^3} \times a_1$$

$$\frac{L_1}{\frac{dL_1}{dt}} \sim \frac{P_2^2}{P_1} \times \frac{m_b + m_2}{m_2} = T_{KL}$$

$$P_1 \ll P_2 \ll T_{KL}$$





$$m_b = m_0 + m_1$$

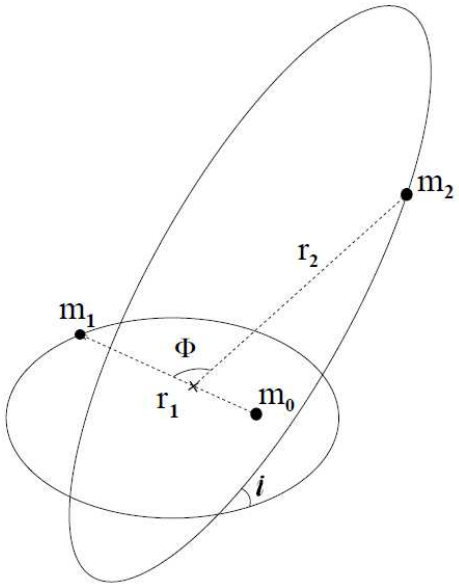
Outline for secular Hamiltonian

Ford et al. 00, Naoz 16, Krymolowski & Mazeh 99
Goldstein 2nd ed

Complete 3-body Hamiltonian (-)

$$\mathcal{F} = \frac{k^2 m_0 m_1}{2a_1} + \frac{k^2 (m_0 + m_1) m_2}{2a_2} + \frac{k^2}{a_2} \sum_{j=2}^{\infty} \alpha^j M_j \left(\frac{r_1}{a_1}\right)^j \left(\frac{a_2}{r_2}\right)^{j+1} P_j(\cos \Phi),$$

$$M_j = m_0 m_1 m_2 \frac{m_0^{j-1} - (-m_1)^{j-1}}{(m_0 + m_1)^j} \qquad k^2 = G$$



Long term evolution of orbital elements (e, I,..)

- Orbital averages for two orbits
- Gravitational interaction of two wires

$a_1 = const, a_2 = const$

$$\mathcal{H} = \mathcal{H}_{quad} + \epsilon_M \mathcal{H}_{oct}$$

$$\mathcal{H}_{quad} = C_2 \{ (2 + 3e_1^2) (3\cos^2 i_{tot} - 1) + 15 e_1^2 \sin^2 i_{tot} \cos(2g_1) \}$$

$$\mathcal{H}_{oct} = -C_2 \frac{15}{4} e_1 \{ A \cos\phi + 10 \cos i_{tot} \sin^2 i_{tot} (1 - e_1^2) \sin g_1 \sin g_2 \}$$

$$C_2 = \frac{G m_0 m_1 m_2}{16 (m_0 + m_1) a_2 (1 - e_2^2)^{3/2}} \left(\frac{a_1}{a_2}\right)^2$$

$$\epsilon_M = \frac{m_o - m_1}{m_0 + m_1} \frac{a_1}{a_2} \frac{e_2}{1 - e_2^2}$$

Example of comparison with direct three body calculation

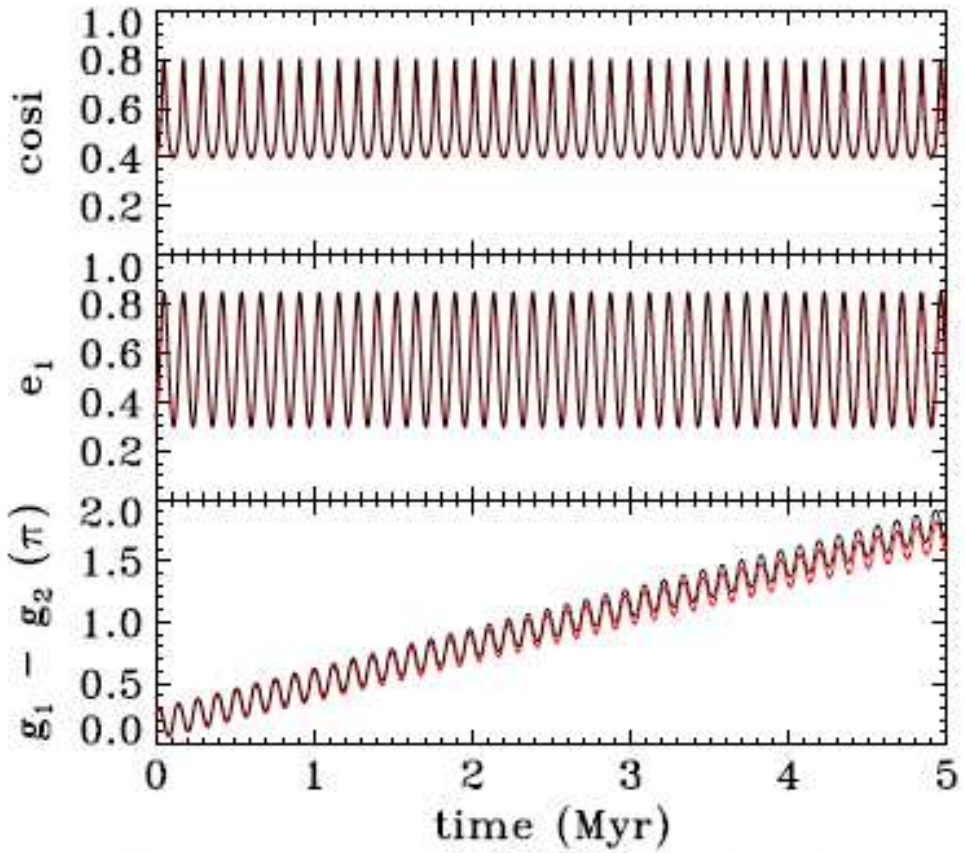
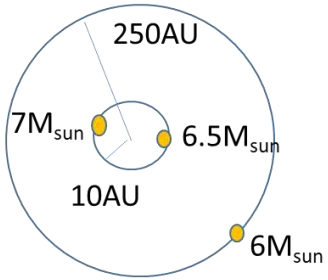


Figure 1. Comparison between our modified FEWBODY code (black) and an octupole-order secular code (red; Blaes et al. 2002). The triple system has $m_0 = 7.0\,M_\odot$, $m_1 = 6.5\,M_\odot$, $m_2 = 6\,M_\odot$, $a_1 = 10$ AU, $a_2 = 250$ AU, $e_1 = 0.3$, $e_2 = 0.1$, $g_1 = 0°$, $g_2 = 0°$, and $\cos i = 0.4$. There is a good agreement between the calculations but there is a slow drift in $g_1 - g_2$. Figure discussed in Section 2.

Black: Direct 3-body calculation
Red: Secular theory

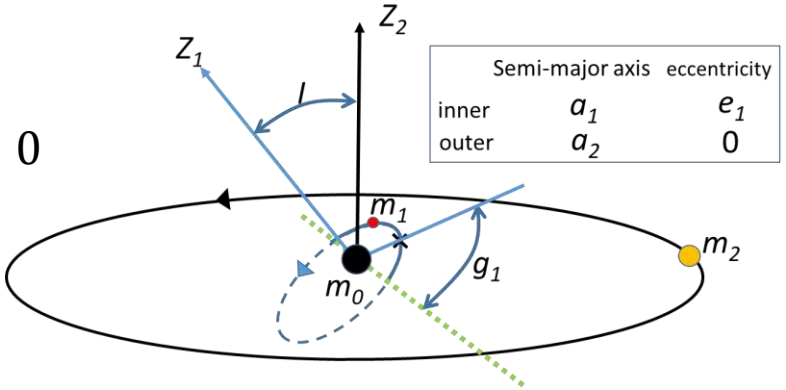


Secular theory: good performance in many cases

Shappee & Thompson 13

$m_1 = 0$ and $e_2 = 0$

$m_1 \to 0$



	Semi-major axis	eccentricity
inner	a_1	e_1
outer	a_2	0

$$\mathcal{H} = \mathcal{H}_{quad} + \epsilon_M \mathcal{H}_{oct}$$

- Outer circular orbit fixed (reference plane)
  - axisymmetric potential: conserve $J_1 \equiv \sqrt{1-e_1^2}\cos I$
- Scaled Hamiltonian

$$H_{quad}(g_1, G_1) = -3G_1^2 - 15\frac{J_1^2}{G_1^2} - 15\,(1-G_2^2)\left(1-\frac{J_1^2}{G_1^2}\right)\cos 2g_1$$

Conjugate variables

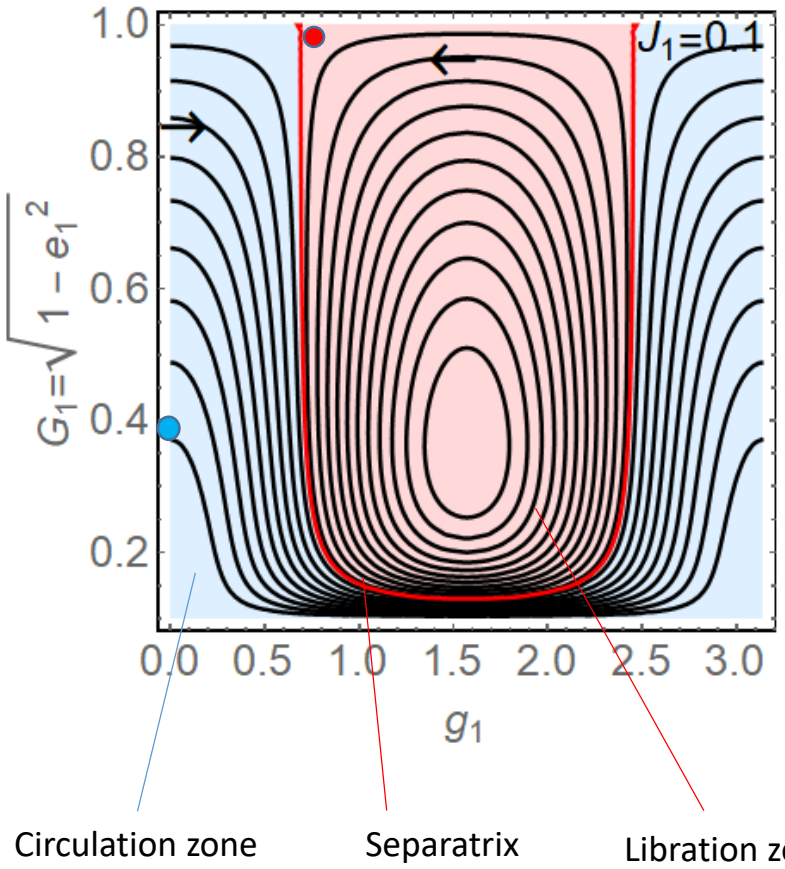
$$G_1 \equiv \sqrt{1-e_1^2}$$

We can learn basic aspects of KL mechanism with this Hamiltonian

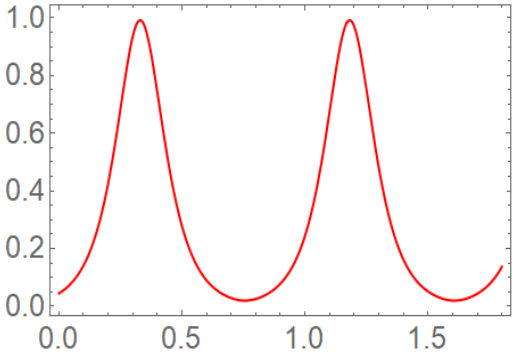
- Eccentricity/inclination oscillation

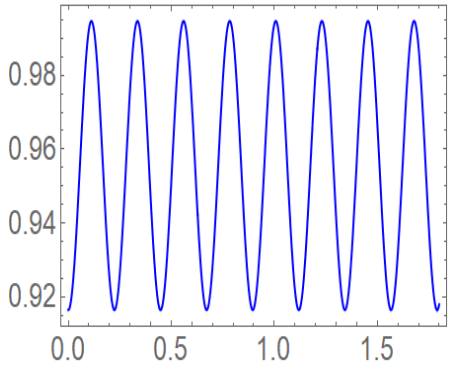
$$J_1 = \sqrt{1 - e_1^2}\cos I = 0.1$$

$$\rightarrow J_1 \leq G_1 \equiv \sqrt{1 - e_1^2} \leq 1$$

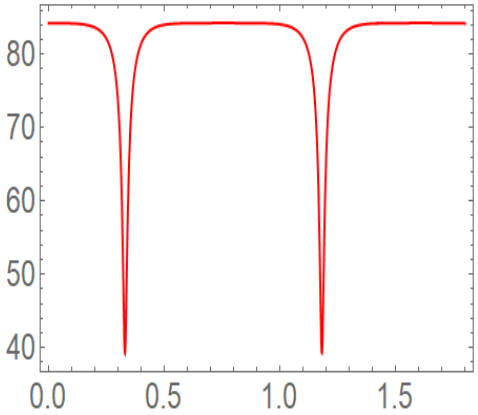


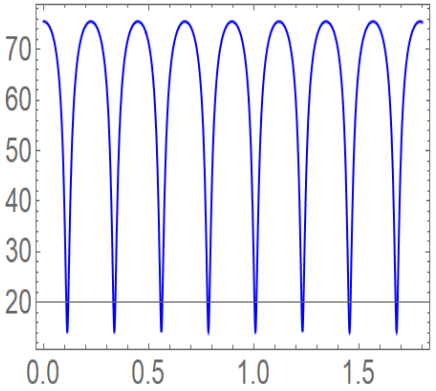
eccentricity



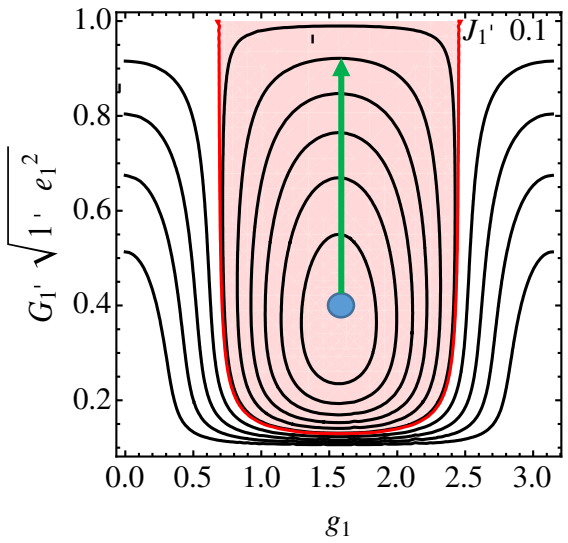


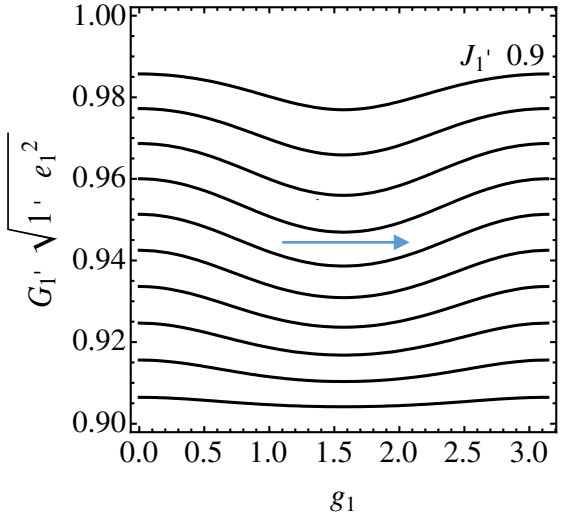
Inclination [degree]





- Existence of libration zone





Critical J_1 for annihilation of the fixed point

$$\frac{\partial H}{\partial G_1}\left(g_1 = \frac{\pi}{2}, G_1 = 1\right) = 0$$

$$\rightarrow J_1 = \sqrt{3/5}$$

$J_1 < \sqrt{3/5}$ Libration + circulation

$J_1 > \sqrt{3/5}$ circulation

$$J_1 = \sqrt{1 - e_1^2}\cos I$$

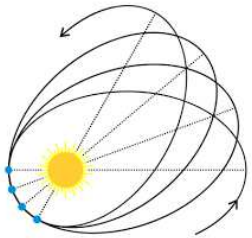
Critical inclination for circular orbit

$$\mathrm{I_{cirit}} = \arccos\sqrt{3/5} = 39.2^o$$

KL suppression by 1PN correction

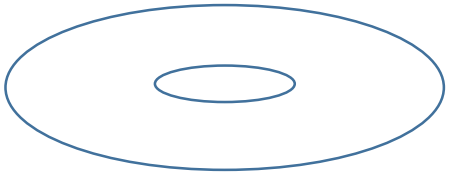
- 1PN apsidal (prograde) precession

$$T_{1PN} = \frac{P_1(1-e_1^2)}{3}\left(\frac{Gm_b}{a_1}\right)^{-1}$$

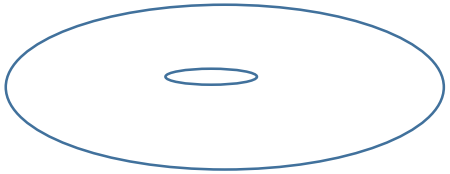


$$H(g_1, G_1) = -3G_1^2 - 15\frac{J_1^2}{G_1^2} - 15\,(1-G_1^2)\left(1-\frac{J_1^2}{G_1^2}\right)\cos 2g_1 + \frac{R}{G_1}$$

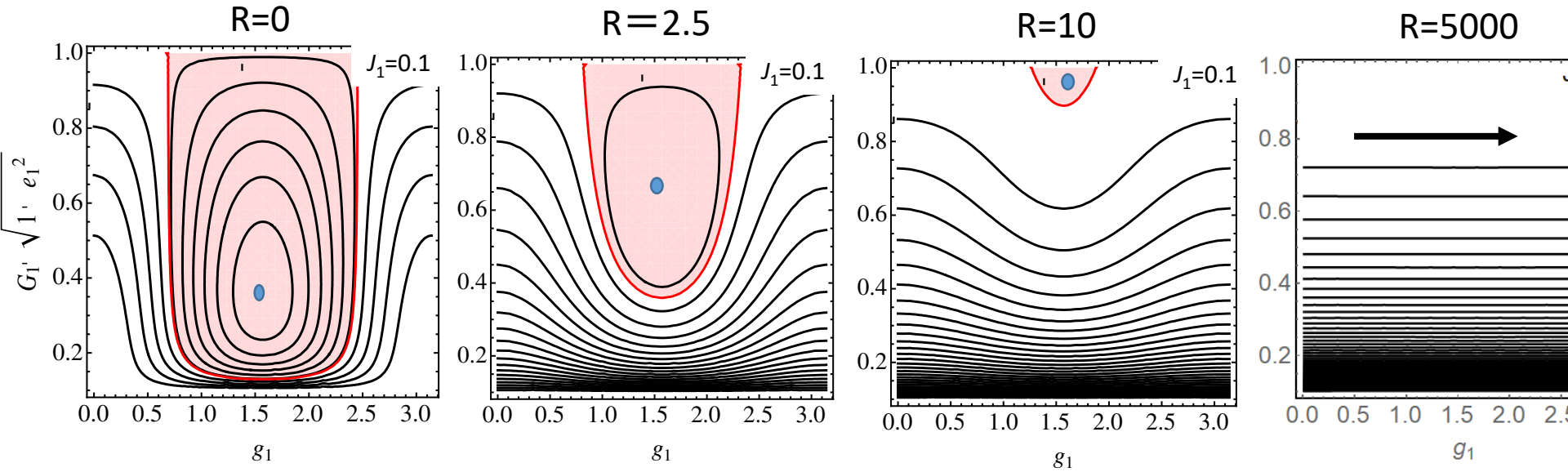
$$R \sim \frac{8}{\pi}\frac{T_{KL}}{T_{1PN}} \propto a_1^{-4}a_2^3$$



smaller R



larger R



$$H(g_1, G_1) = -3G_1^2 - 15\frac{J_1^2}{G_1^2} - 15\,(1 - G_1^2)\left(1 - \frac{J_1^2}{G_1^2}\right)\cos 2g_1 + \frac{R}{G_1}$$

- larger R : stronger prograde precession
  - Libration zone shrinks
  - Eccentricity oscillation decreases
- annihilation of the fixed point

$$\frac{\partial H}{\partial G_1}\left(g_1 = \frac{\pi}{2}, G_1 \to 1\right) = 0$$

$$R = 12 - 20J_1^2$$

Some of recent studies on KL

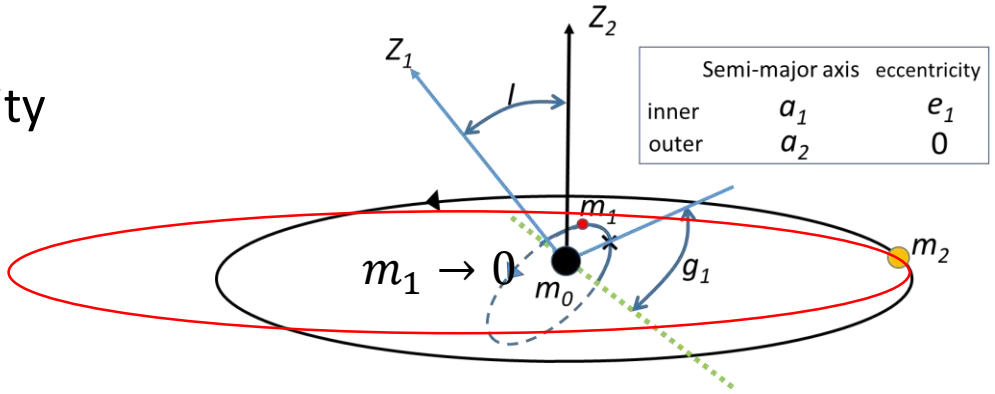
- Realize highly eccentric orbits (e.g. for rapid evolution)
  - Eccentric KL (EKL) by octupole term
  - Validity of double averagings
- Activate eccentricity amplification after binary evolution
  - mass loss induced EKL
  - Velocity related effects (WD kick, flyby)
- 3-body systems in dense star clusters

Eccentric KL (EKL) mechanism

- Effects of outer eccentricity $e_2 \neq 0$ (octupole term)

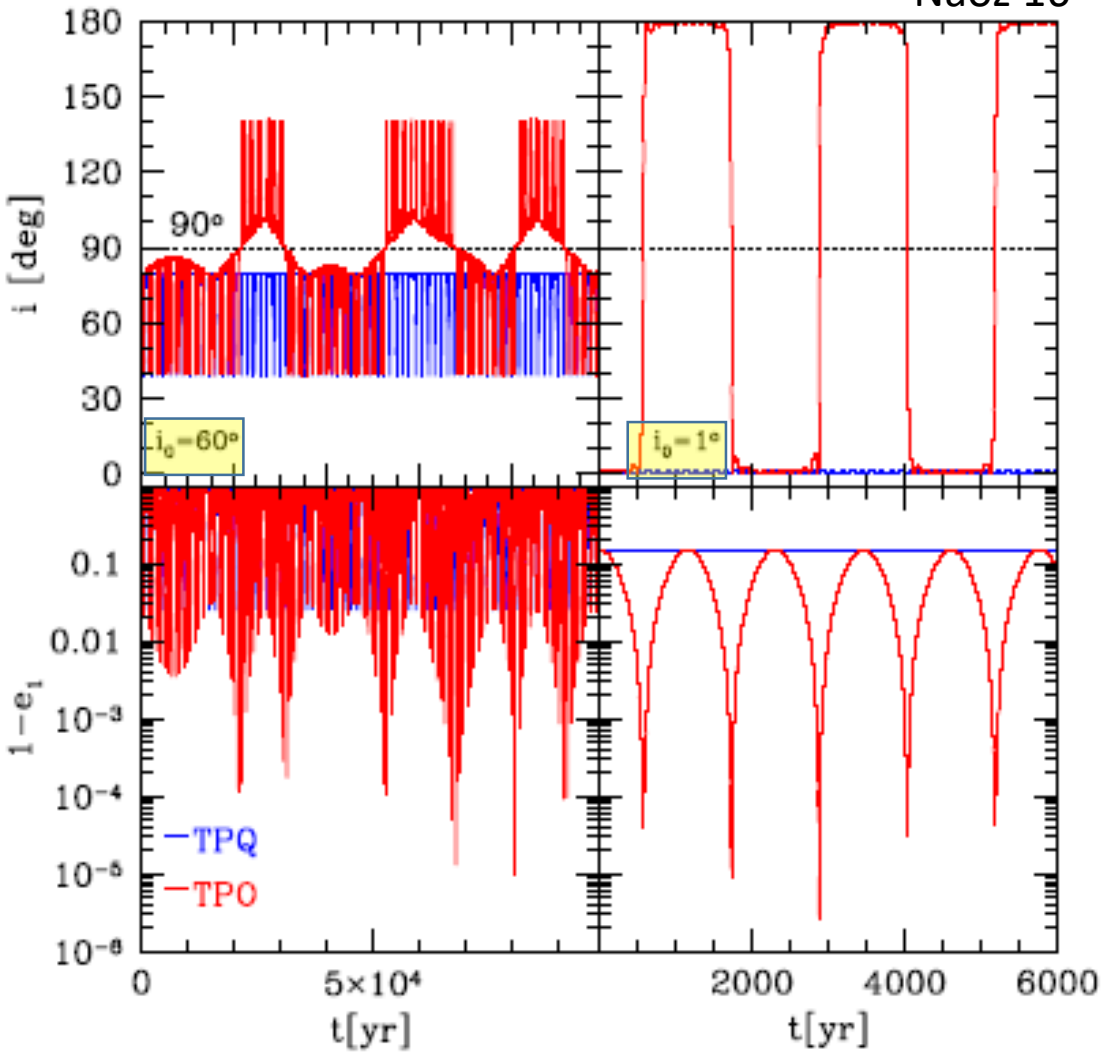
$$H_{quad} + \epsilon_M H_{oct} \qquad \epsilon_M = \frac{m_1 - m_2}{m_1 + m_2} \frac{a_1}{a_2} \frac{e_2}{1 - e_2^2}$$

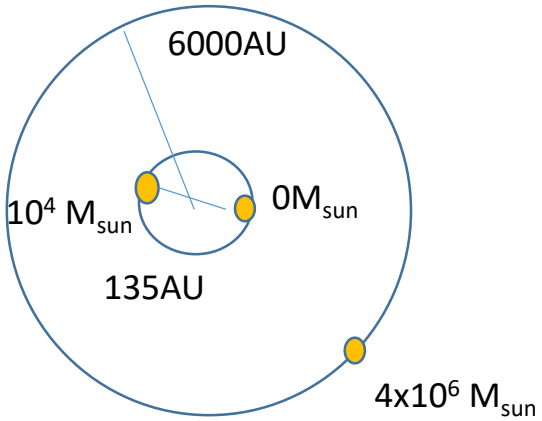
- Even test particle case
  - J_1 not conserved
    - Larger eccentricity
    - Orbital flip



Lithwick & Naoz 11, Naoz 16

Naoz 16





e_2=0.7

Highly eccentric even with i<<39°

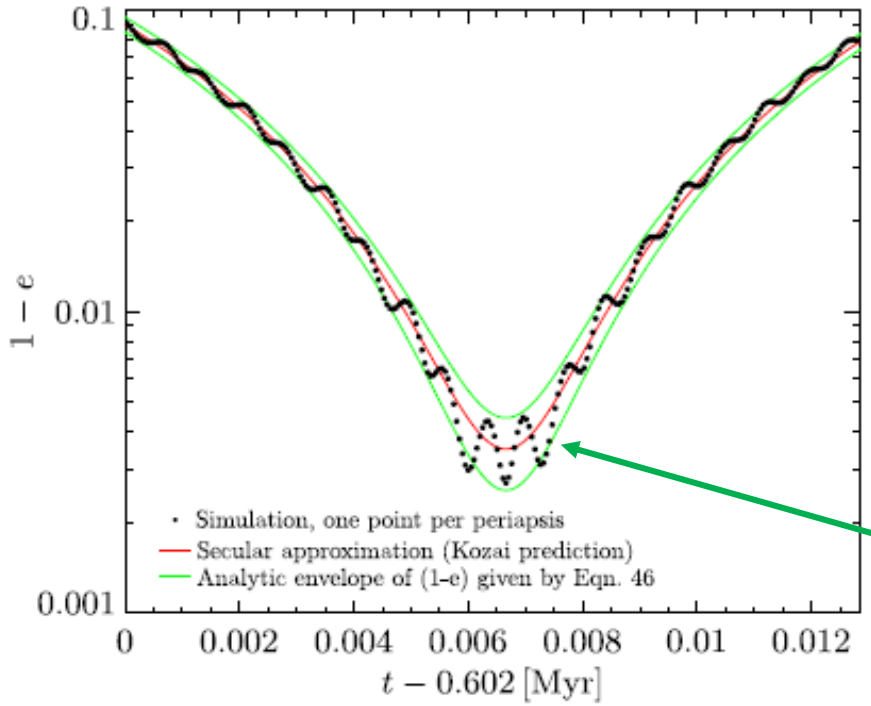
Time evolution example of the TPO (test partial octupole) approximation (red lines) and the TPQ (test particle quadrupole) approximation (blue lines). *Left panels* show high inclination flip while the *right panels* show the low inclination flip (see text). In this example we consider the time evolution of a test particle at 135 AU around a 10^4 $M_\odot$ intermediate black hole located 0.03 pc from the massive black hole in the center of our galaxy (4×10^6 $M_\odot$). In the left panels the system initially is set with $e_1 = 0.01$, $e_2 = 0.7$, $i = 60°$, $\Omega_1 = 60°$ and $\omega_1 = 0°$. In the right panels the system is initially set with $e_1 = 0.85$, $e_2 = 0.85$, $i = 1°$, $\Omega_1 = 180°$ and $\omega_1 = 0°$. In the top panels we show the inclination and in the bottom the inner orbit eccentricity as $1 - e_1$.

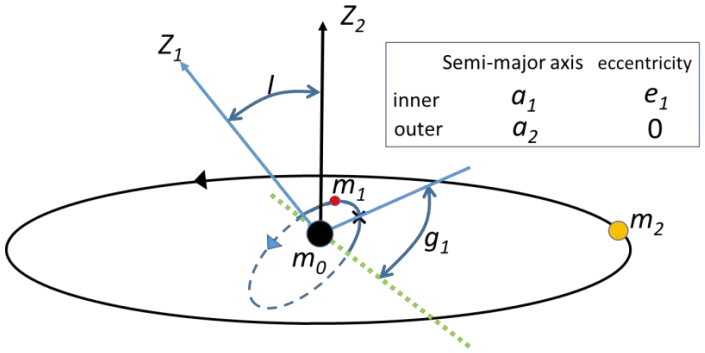
Validity of double averaging

(Ivanov et al. 05, Antonini & Perets 12, Katz & Dong 12, Bode & Wegg 14, Antonini et al. 14, Antognini et al. 14)

Fluctuation of inner angular momentum in one outer orbital period P_2

Bode & Wegg 14





$$\Delta L_1 \sim \frac{G m_2 a_1}{a_2^3} \times a_1 \times \frac{P_2}{4}$$

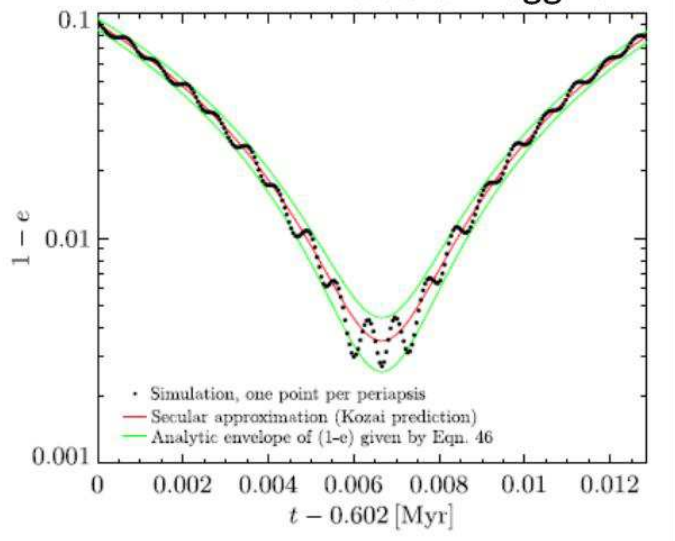
"coherent time"

- Double averagings work for $\Delta L_1 \ll L_1$

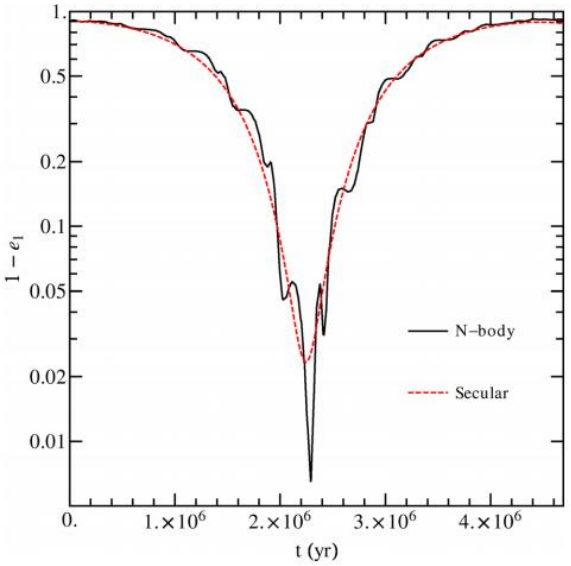
- Double averagings do not work for $\Delta L_1 \gtrsim L_1$
  - could be highly eccentric

$$1 - e_1 \lesssim \left(\frac{a_1}{a_2}\right)^3 \frac{m_2^2}{m_b(m_b+m_2)}$$

Bode & Wegg 2014



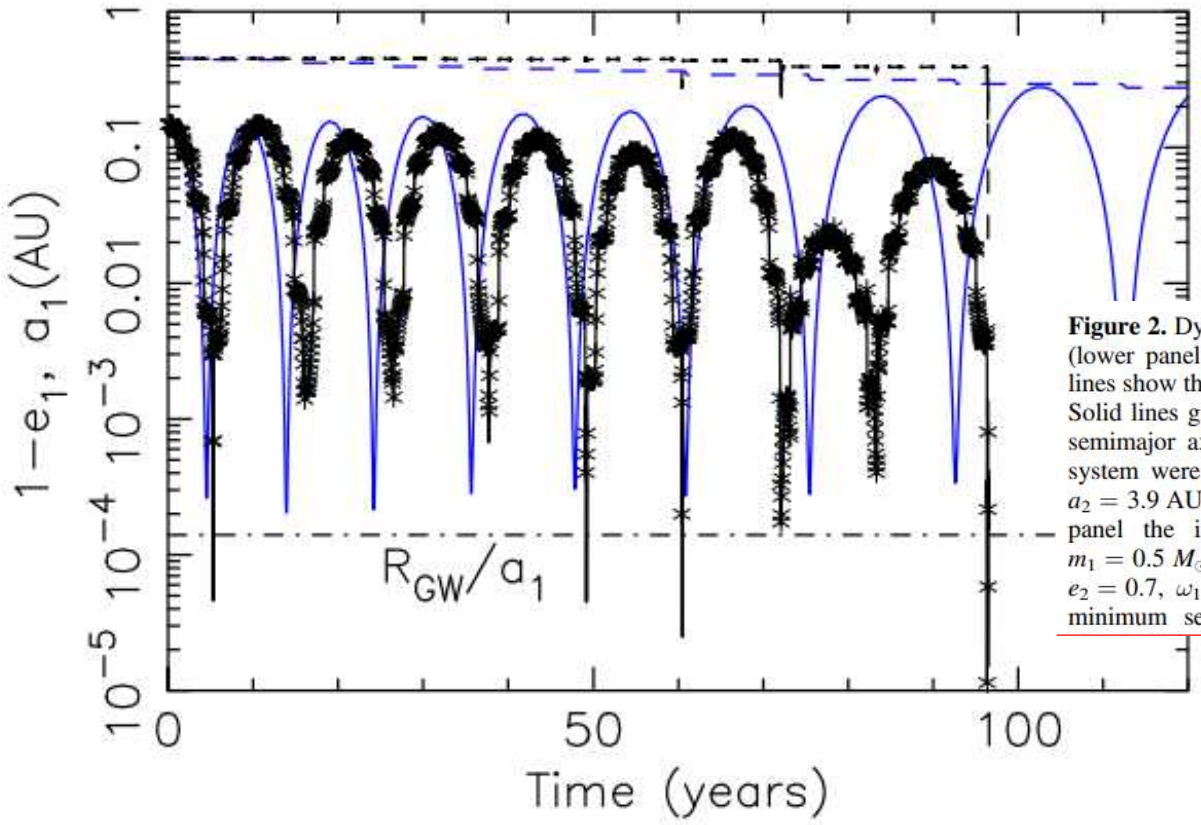
Antognini et al. 16



Ex1: GW from binary merger

(Antonini & Perets 12, Seto 13, Antonini et al. 14, Antognini et al. 14,Antonini et al. 16, Gupta et al.19)

- $\Delta E \propto (1-e)^{-3.5}$
- Comparison between secular theory and direct PN 3body



Black: direct 3-body

Blue: octpole+GW

Figure 2. Dynamical evolution of a BH triple (upper panel) and a stellar triple (lower panel). Black lines show the results of three-body integrations, blue lines show the results of the octupole order orbit averaged equations of motion. Solid lines give the value of $(1 - e_1)$, and dashed lines give the inner binary semimajor axis. In the upper panel the initial conditions for the BH triple system were: $m_0 = 14.9\ M_\odot$, $m_1 = 13.8\ M_\odot$, $m_2 = 14.2\ M_\odot$ $a_1 = 0.45$ AU, $a_2 = 3.9$ AU, $e_1 = 0.85$, $e_2 = 0.51$, $I = 92.^\circ5$, $\omega_1 = \omega_2 = \pi/2$. In the lower panel the initial conditions for the stellar triple were: $m_0 = 0.7\ M_\odot$, $m_1 = 0.5\ M_\odot$, $m_2 = 2\ M_\odot$ $a_1 = 1$ AU, $a_2 = 25$ AU, $I = 101.^\circ8$, $e_1 = 0.1$, $e_2 = 0.7$, $\omega_1 = 214.^\circ6$, $\omega_2 = 0$. In the upper panel the asterisks denote the minimum separation attained by the two BHs every orbital period. At

Antonini et al. 16

Antonini et al. 2014

BBH Residual eccentricity distribution

larger than expected before!

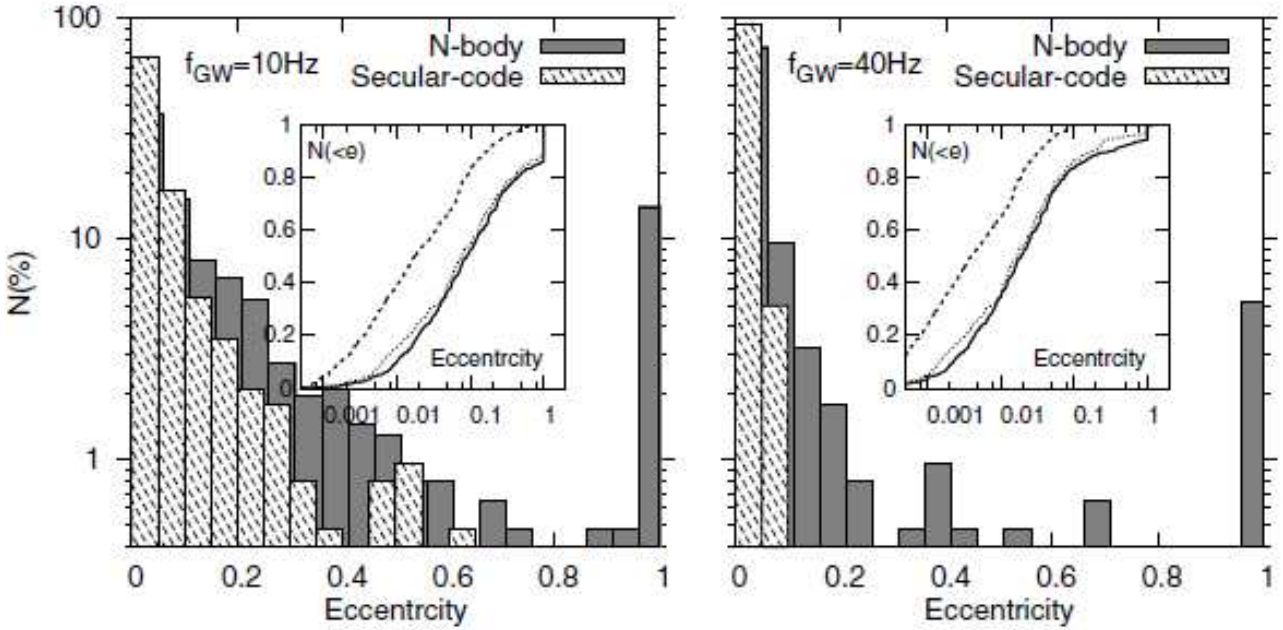
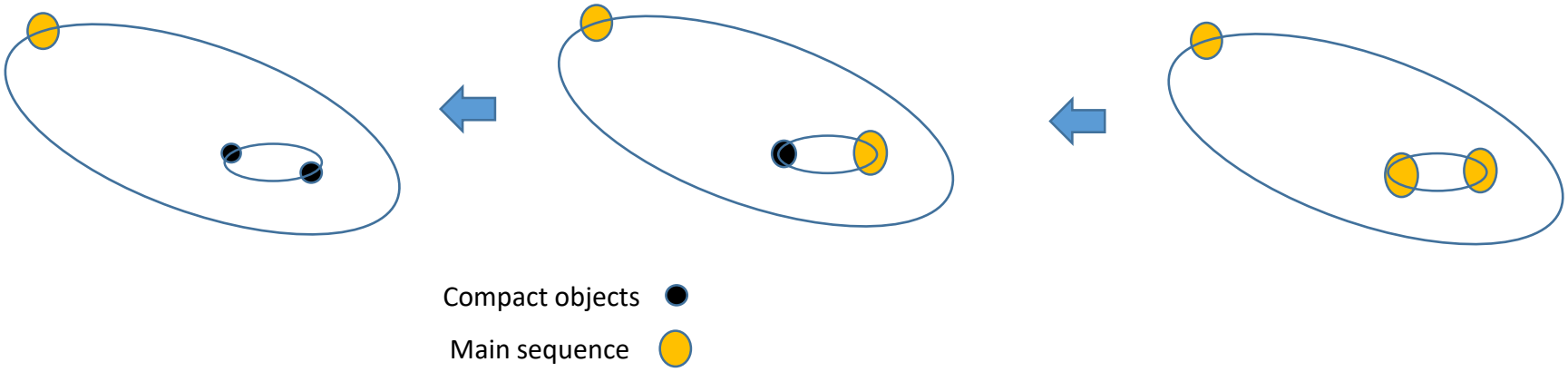


Figure 5. Histograms of the eccentricity distribution in MOD1 of coalescing BH binaries driven by the Kozai mechanism in GCs when their emitted GW signal first enters the 10 Hz (left panel) and the 40 Hz (right panel) frequency bands. Insert panels show the corresponding cumulative distribution of eccentricities. Distributions are normalized to the total number of systems that merge before being perturbed by encounters with other stars in the cluster. Systems were evolved using both the octupole-order orbit average equations of motion (hatched histograms and dashed lines) and more accurate three-body direct integrations (filled histograms and solid lines). The three-body runs produce orbital distributions that are significantly more biased toward large eccentricities; they predict that about 50% of merging binaries have eccentricities larger than 0.1 and that 10% of them posses extremely large eccentricities ($e_1 \sim 1$) when they first enter the aLIGO frequency band. The number of these highly eccentric GW sources is strongly underestimated when using the orbit average (secular) code. Dotted lines in the insert panels give the cumulative distribution of eccentricities of coalescing BH binaries in MOD1-bis. In this model the three-body initial conditions were sampled from the entire distribution corresponding to MOD1, instead of being selected on the basis of Equation (21).

Some of recent studies

- Realize highly eccentric orbits (e.g. for rapid evolution)
  - Eccentric KL (EKL) by octupole term
  - Validity of double averaging
- Activate eccentricity amplification after binary evolution
  - mass loss induced EKL
  - Velocity related effects (WD kick, flyby)
- 3-body systems in dense star clusters

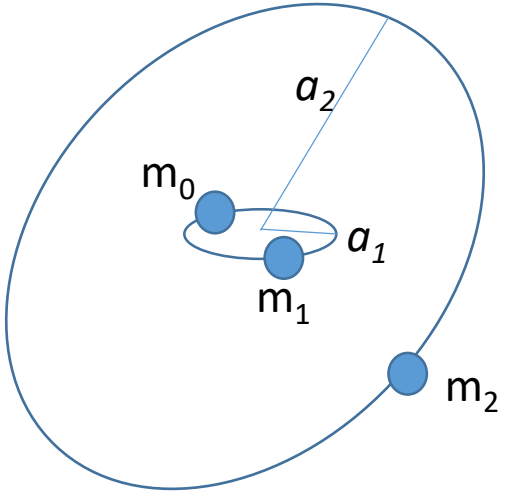


Mass loss induced eccentric KL

Shappee &Thompson 2013, Naoz et al. 2015

$$H_{quad} + \epsilon_M H_{oct}$$

$$\epsilon_M = \frac{m_o - m_1}{m_0 + m_1}\frac{a_1}{a_2}\frac{e_2}{1-e_2^2}$$

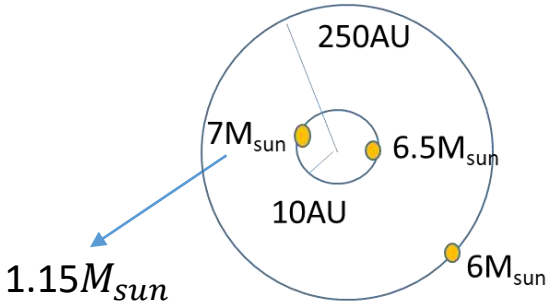


Increase ϵ_M by mass loss of m_0

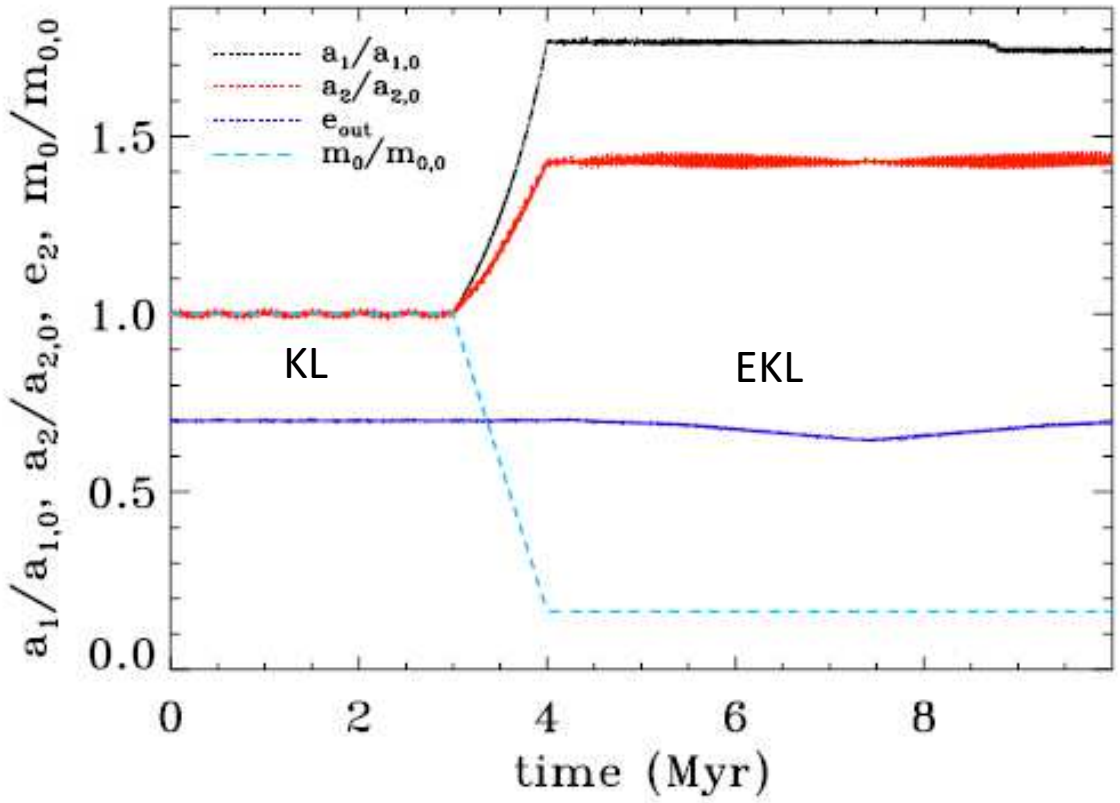
- Enhance the mass asymmetry of inner binary
  - $m_0 \sim m_1 \quad \rightarrow m_1 \gg m_0$
- Increase a_1/a_2 by mass loss (minor effect)

  Adiabatic and isotropic mass loss

$$\frac{a_1}{a_2} \propto \frac{m_0 + m_1 + m_2}{m_0 + m_1}$$



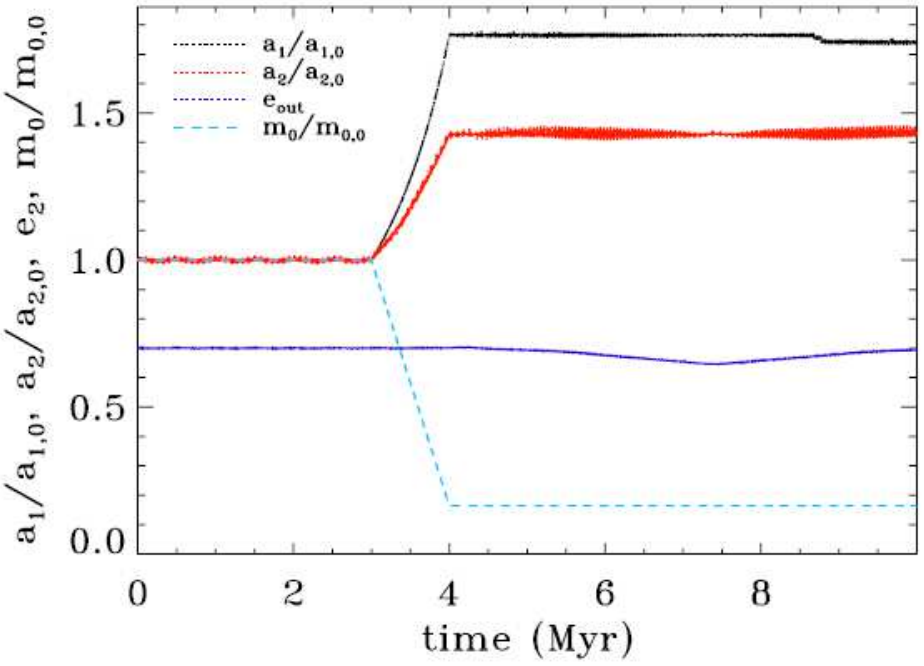
$e_1 = 0.1 \;\; e_2 = 0.7$

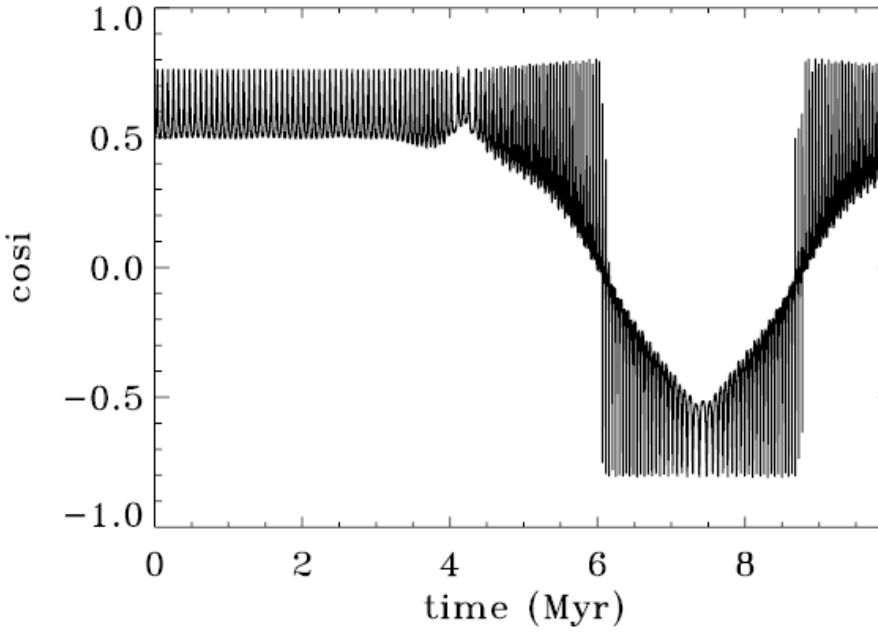


$$H_{quad} + \epsilon_M H_{oct}$$

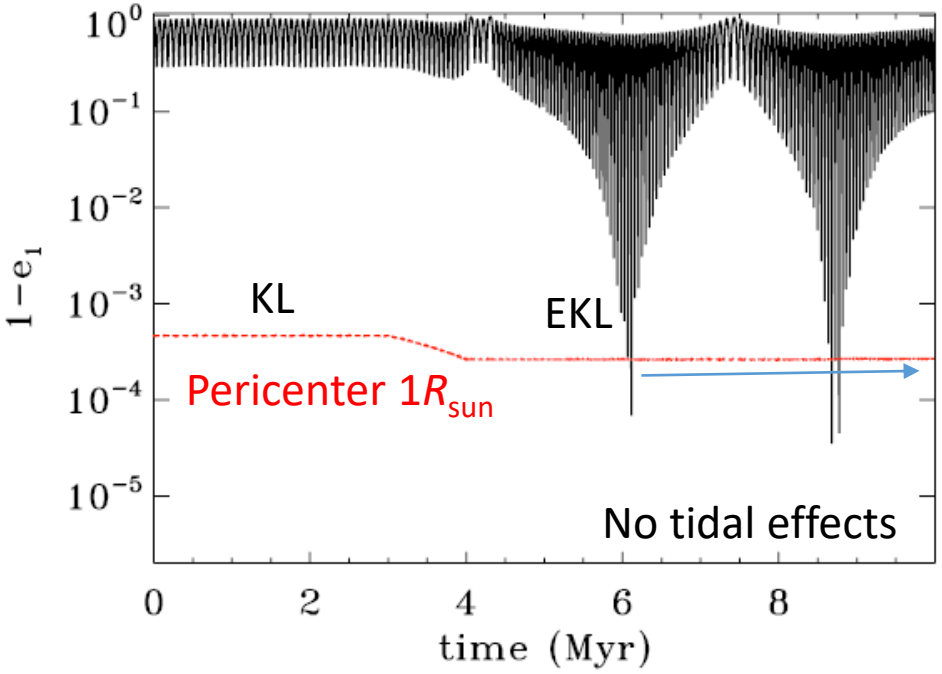
$$\epsilon_M = \frac{m_o - m_1}{m_0 + m_1} \frac{a_1}{a_2} \frac{e_2}{1 - e_2^2}$$

$$\epsilon_M = 0.002 \rightarrow 0.047$$

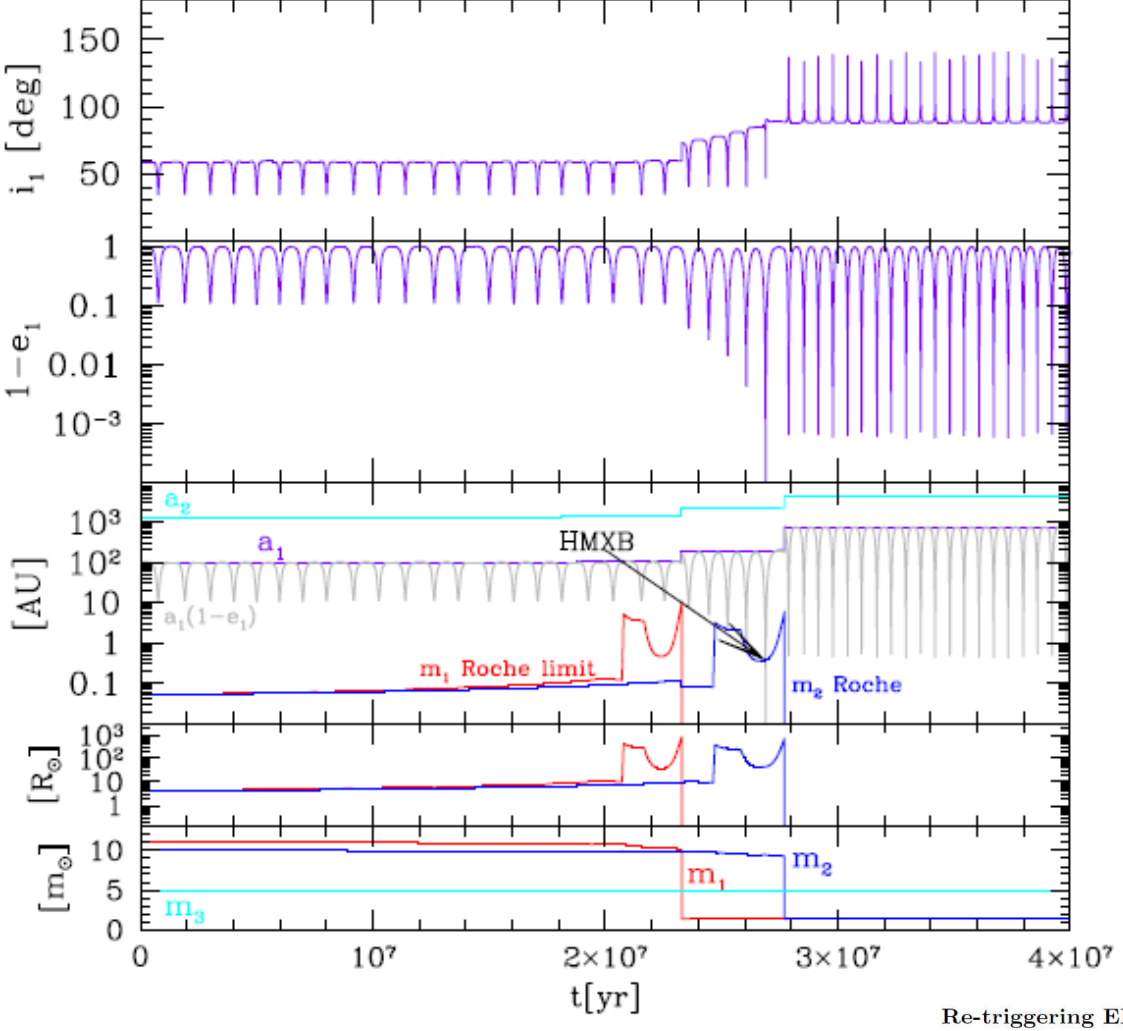




Shappee &Thompson 2013



Highly eccentric 1-e=0.3 → 0.0001
tidal interaction



Naoz 2016

$11M_{sun}$ +$10M_{sun}$+$5M_{sun}$

100AU 1300AU

$1.4M_{sun}$ NS without kick

$\epsilon_M = 0.0034 \rightarrow 0.061$

HMXB, Thorne-Zytkow object,…

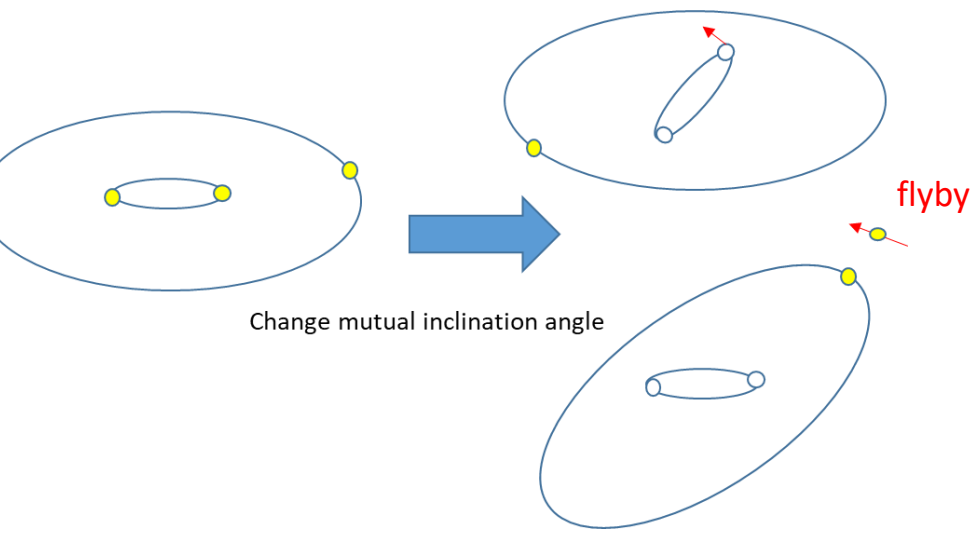
Re-triggering EKL by mass loss. This example produces a High Mass X-ray Binary (HMXB) or a supernova impostor. We show (top to bottom) the inner orbit inclination i_1, the inner orbit eccentricity (depicted as $1 - e_1$), the semi-major axis of the inner (purple) and outer (cyan) orbit as well as the inner orbit peri-center and the two masses disruption distances (see Eq. (54) for a popular definition), the stellar radii and finally the bottom panel shows the masse of all three stars. This calculation includes solving the equations of the octupole-level of approximation, GR for both the inner and outer orbit, and stellar evolution according to SSE (Hurley et al. 2000), which includes mass loss and staler inflation. For simplicity the supernova was modeled here as a simple mass loss and assuming no kicks. Tidal evolutions were turned of for illustration purposes. A consequence of the first mass loss episode and the formation of a neutron star is that the initially small ϵ_M increased. This yields eccentricity excitations leading to Roche limit crossing as the m_2 star's radius inflates . This may result in a HMXB, or even a supernova impostor. The system parameters are set initially: $m_1 = 11$ $M_\odot$, $m_2 = 10$ $M_\odot$, $m_3 = 5$ $M_\odot$, $a_1 = 100$ AU, $a_2 = 1300$ AU, $e_1 = 0.001$, $e_2 = 0.6$, $\omega_1 = \omega_2 = 0$ and $i_{\rm tot} = 79°$. These parameters yield initial $\epsilon_M = 0.0034$. Naoz et al. (2015) discussed the formation scenario of low mass X-ray binaries via triple body evolution similarly to the example illustrated here.

WD kick and stellar flyby for type 1a

Hamers & Thompson 2019

- Change mutual inclination angle
- Activate KL later for SN1a by WD-WD merger

hypothetical WD kick O(1km/sec)



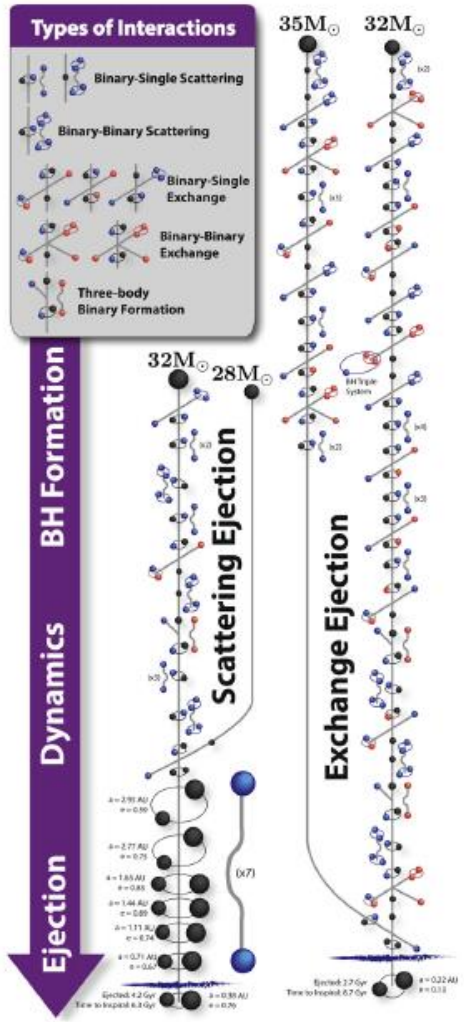
Enhance KL induced merger?
Disrupt three body systems?

Population synthesis study

SNIa rate 1.1×10^{-4} M^{-1}_{sun} with WD kick +flyby

- 2.5 time larger than without WD kick + flyby
- Still 10 time smaller than the observed rate
- Large uncertainities

Dynamical formation of hierarchical triple systems in dense star clusters

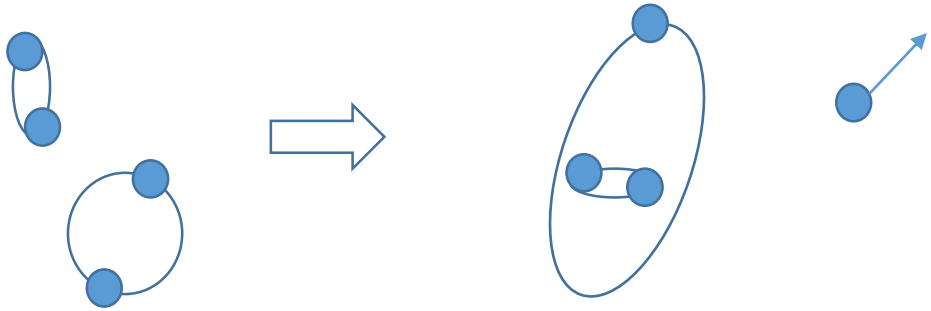


Rodriguez et al. 16

LIGO sources produced as ejected binaries



Binary-binary interaction (Miller & Hamilton 02)



Cluster simulation results for KL

Antonini et al. 16

Source	Detection Rates (yr^{-1})		
	Low	Realistic	High
Hierarchical triples	0.11	0.47	1.9
Eccentric inspirals (e>0.1 f=10Hz)	0.021	0.20	0.48
In-cluster mergers	0.011	0.062	0.60
Dynamically formed binary	10	30	100

KL

- KL merger: ~1% of dynamically formed events
  - mostly within clusters
  - Large residual eccentricity in LIGO band

Summary

- Orbital stability
  - Hierarchy for mass or separations
- 1:0 resonance supported by PN apsidal precession
  - Special mean motion resonance for hierarchical orbits
- Kozai-Lidov mechanism
  - Secular Hamiltonian
    - Captures basic aspects of KL
    - Suppression by 1PN apsidal precession
  - How to realize $1-e \ll 1$?
    - Eccentric Kozai-Lidov (EKL)
    - breakdown of double averagings
  - How to KL along with stellar evolution?
    - Mass loss induced EKL, WD kick + flyby
  - Formation of hierarchical three body systems in dense star clusters
    - Rate: ~1/100 of ejected binaries but highly eccentric ones 、